

GT2011-45213

FRICION FACTOR BEHAVIOR FROM FLAT-PLATE TESTS OF 12.15 mm DIAMETER HOLE-PATTERN ROUGHENED SURFACES

Thanesh Deva Asirvatham
Graduate Research Assistant,
Texas A&M University,
College Station, TX 77843 USA
e-mail: thaneshda@gmail.com

Dara W. Childs
Turbomachinery Laboratory,
Texas A&M University,
College Station, TX 77843 USA
e-mail: dchilds@tamu.edu

Stephen Phillips
Turbomachinery Laboratory,
Texas A&M University,
College Station, TX 77843 USA
e-mail: sphillips@tamu.edu

ABSTRACT

A flat-plate tester is used to measure the friction-factor behavior for a hole-pattern-roughened surface facing a smooth surface with compressed air as the medium. Measurements of mass flow rate, static pressure drop and stagnation temperature are carried out and used to find a combined (stator + rotor) Fanning friction factor value. In addition, dynamic pressure measurements are made at four axial locations at the bottom of individual holes of the rough plate and at facing locations in the smooth plate. The description of the test rig and instrumentation, and the procedure of testing and calculation are explained in detail in Kheireddin in 2009 and Childs et al. in 2010.

Three hole-pattern flat-plates with a hole-pattern diameter of 12.15 mm were tested having depths of 0.9, 1.9, and 2.9 mm. Tests were done with clearances at 0.254, 0.381, and 0.653 mm, and inlet pressures of 56, 70 and 84 bar for a range of pressure ratios, yielding a Reynolds-number range of 100,000 to 800,000. The effects of Reynolds number, clearance, inlet pressure, and hole depth on friction factor are studied.

The data are compared to friction factor values of three hole-pattern flat-plates with 3.175 mm diameter holes with hole depths of 1.9, 2.6, and 3.302 mm tested in the same rig described by Kheireddin in 2009.

The test program was initiated mainly to investigate a “friction-factor jump” phenomenon cited by Ha et al. in 1992 in test results from a flat-plate tester using facing hole-pattern plates where, at elevated values of Reynolds numbers, the friction factor began to increase steadily with increasing Reynolds numbers. Friction-factor jump was not observed in any of the current test cases.

Keywords: Friction factor, flat plate testing, annular gas seals

INTRODUCTION

Annular seals with a smooth rotor and a hole-pattern (HP) stator are used commonly in high pressure compressors. For small motions of the rotor about a centered position, the rotor seal reaction force is:

$$-\begin{Bmatrix} F_X \\ F_Y \end{Bmatrix} = \begin{bmatrix} K(\Omega) & k(\Omega) \\ -k(\Omega) & K(\Omega) \end{bmatrix} \begin{Bmatrix} X \\ Y \end{Bmatrix} + \begin{bmatrix} C(\Omega) & c(\Omega) \\ -c(\Omega) & C(\Omega) \end{bmatrix} \begin{Bmatrix} \dot{X} \\ \dot{Y} \end{Bmatrix} \quad (1)$$

Here, X and Y are the displacements of the rotor relative to the seal, and F_X and F_Y are the components of the reaction forces acting on the rotor in the X and Y directions, respectively. K is the direct stiffness, k is the cross-coupled stiffness, C is the direct damping, and c is the cross-coupled damping. K , k , C and c are the rotordynamic coefficients. Kleynhans and Childs [4] predicted, and subsequent tests have shown that the rotordynamic coefficients for HP-stator seals can be strongly frequency dependent.

Friction factor data are important in predicting seal leakage and also in developing more correct partial derivatives of friction factor with clearance and Reynolds number in predicting rotordynamic coefficients [4, 5]. A flat-plate test rig can be used to obtain friction factor data for seal configurations. Kheireddin [1] tested flat-plates with hole-pattern diameter of 3.175 mm. A hole-pattern diameter of 12.15 mm diameter was selected to establish friction factor data for larger diameter hole pattern seals and to serve as a basis to decide on the optimum HP geometries for better leakage control. These experimental friction factor data can also serve as a basis for CFD simulations

NOMENCLATURE

A	Cross sectional area of the flow path [L ²]
C, c	Direct and cross-coupled damping coefficients [FT/L]
C_{pl}	Clearance between plates [L]
f_f	Fanning friction factor
\bar{f}_f	Reynolds number based averaged Fanning friction factor
h_d	Hole depth [L]
h_ϕ	Hole diameter [L]
K, k	Direct and cross-coupled stiffness coefficients [F/L]
M	Mach number
\dot{m}	Mass flow rate [M/T]
P	Static pressure [F/L ²]
P_{in}	Inlet pressure [F/L ²]
R	Gas constant [FL/M Kelvin]
Re	Reynolds Number
T	Static temperature [Kelvin]
T_t	Stagnation temperature [Kelvin]
V	One dimensional fluid velocity [L/T]
W	Plate width [L]
γ	Ratio of specific heats
γ_A	Area ratio

CALCULATING FRICTION FACTORS FROM FLAT-PLATE TEST DATA

The procedure used to calculate the friction factor is based on the Fanno-line solution for compressible flow in rectangular channels as documented by John [6]. The Mach number M is related to the fluid velocity V by

$$M = \frac{V}{\sqrt{\gamma RT}} \quad (2)$$

where γ is the ratio of specific heats, R is the gas constant, and T is the static temperature. The following equation for M is derived from conservation of mass, the ideal gas law, and the stagnation temperature.

$$M = \left(\frac{-1 + \sqrt{1 + 2(\gamma - 1) \left(\frac{\dot{m}}{PA} \right)^2 \left(\frac{RT_t}{\gamma} \right)}}{(\gamma - 1)} \right)^{\frac{1}{2}} \quad (3)$$

\dot{m} is the mass flow rate through the test section. $A = WC_{pl}$ is the cross-sectional area of the rectangular channel in the

tester, where C_{pl} is the plate clearance and W is the flow area width. Further, T_t is the stagnation temperature, defined by

$$T_t = T \left(1 + \frac{\gamma - 1}{2} M^2 \right) \quad (4)$$

In Eq. (3), \dot{m} , P , and T_t are measured quantities, whereas, R , γ and A are known, making the M calculation fairly simple.

The friction factor is given by,

$$f_f = \frac{C_{pl}(1 - M^2)}{\gamma M^3 \left(1 + \frac{\gamma - 1}{2} M^2 \right)} \frac{dM}{dx} \quad (5)$$

where dM/dx is the Mach-number gradient, and x is the axial coordinate along the plate's axis.

TEST RIG AND TEST PROCEDURE

Detailed descriptions of the test rig, instrumentation, plate-assembly procedure, test procedure, data reduction, and calculation procedure are provided by Kheireddin [1] and Childs et al. [2]. A detailed view of flat-plate tester is shown in Fig. 1 and the flow loop is shown in Fig. 2.

TEST PLATES

Figure 3 shows one of the tested plates. γ_A is the ratio of area occupied by holes to the total surface area. For the plates tested, $\gamma_A = 75.4\%$. The rough plate has nine static pressure measurement locations and four dynamic pressure locations. The smooth plate has two static sensor locations for each inlet and exit pressure measurements, plus inlet and exit temperature probes and four dynamic pressure sensors.

Figure 4 shows the flat-plate tested earlier, with hole pattern of diameter 3.175 mm that had $\gamma_A = 68.1\%$.

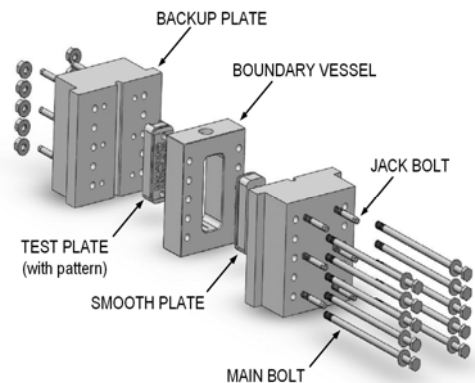


Figure 1. Detailed view of the flat-plate tester

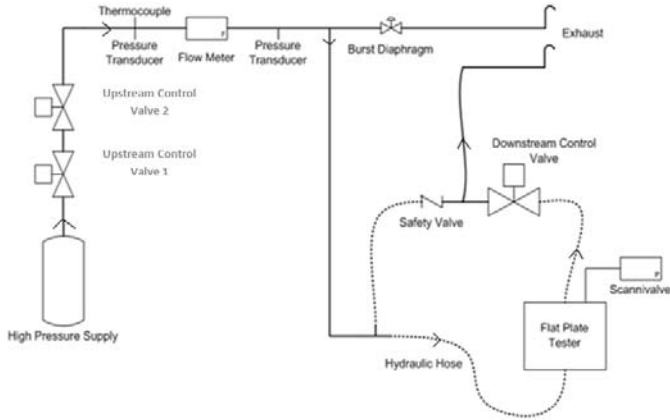


Figure 2. Flow loop

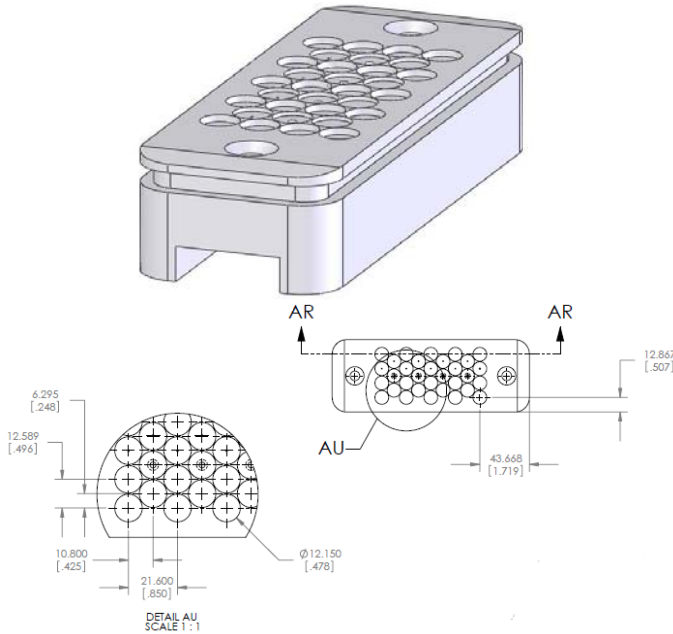


Figure 3. Flat-plate used for the current study with hole-pattern diameter of 12.15 mm (Dimensions are in mm)

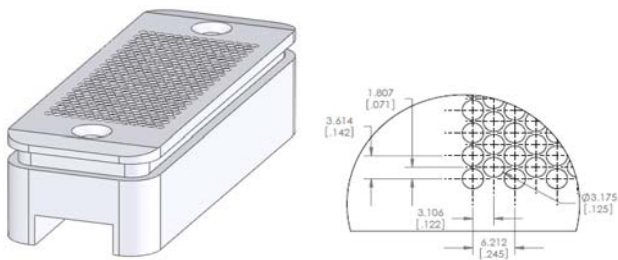


Figure 4. Flat-plate with hole-pattern diameter of 3.175 mm (Dimensions are in mm)

TEST CONDITIONS

Tests were performed at the 27 conditions cited in Table 1. f_f was calculated for a range of pressure ratios at each test condition.

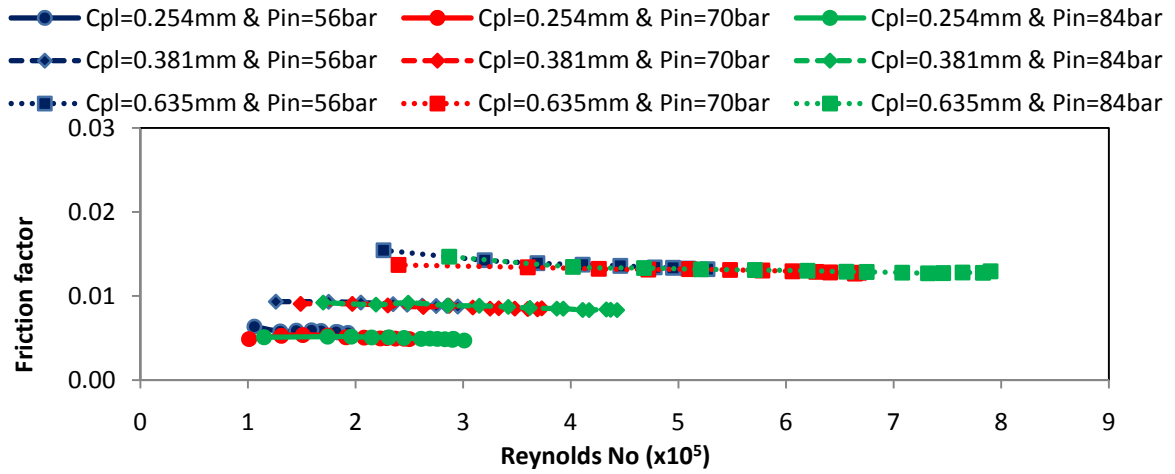
Table 1. Test configurations

Sl.No.	Hole depth	Clearance	Inlet
1	0.9	0.254	56
2			70
3			84
4		0.381	56
5			70
6			84
7		0.635	56
8			70
9			84
10	1.9	0.254	56
11			70
12			84
13		0.381	56
14			70
15			84
16		0.635	56
17			70
18			84
19	2.9	0.254	56
20			70
21			84
22		0.381	56
23			70
24			84
25		0.635	56
26			70
27			84

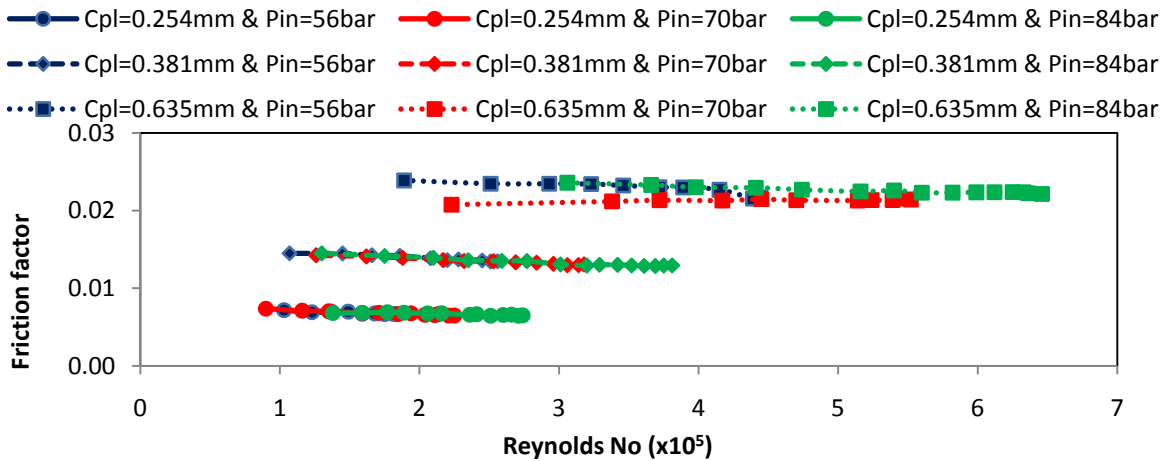
FRICITION FACTOR DATA

Friction factor data versus Re are presented in Fig. 5 for all the tests.

(a) Friction factor Vs. Re for $h_d = 0.9$ mm



(b) Friction factor Vs. Re for $h_d = 1.9$ mm



(c) Friction factor Vs. Re for $h_d = 2.9$ mm

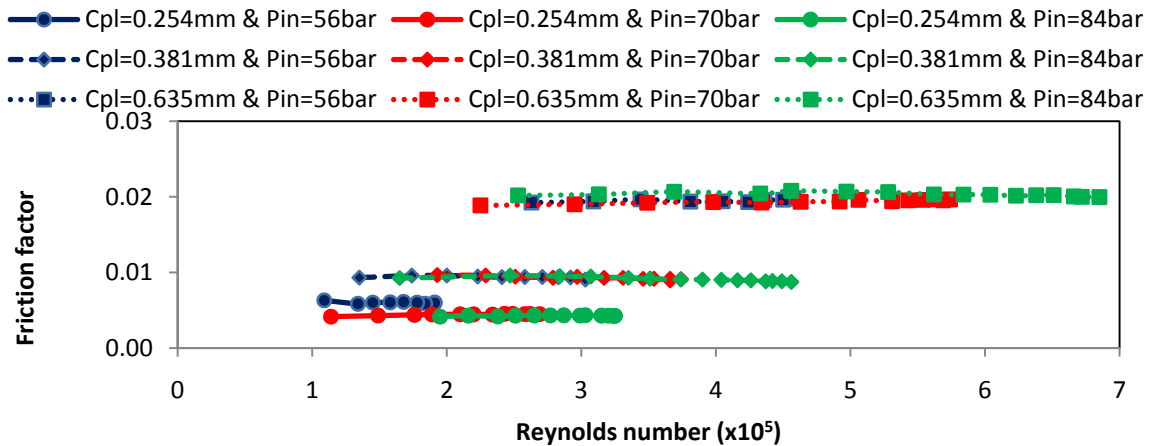


Figure 5. Friction factor data versus Re for $h_\phi = 12.15$ mm with (a) $h_d = 0.9$, (b) $h_d = 1.9$, and (c) $h_d = 2.9$ mm

Reynolds-number Influence

The following observations can be made from Fig.5.

- For $h_d = 0.9$ mm, f_f decreases with increasing Re .
- For $h_d = 1.9$ mm, at low clearances, f_f decreases with increasing Re . At the larger C_{pl} value of 0.635 mm, f_f hardly changes with respect to increasing Re .
- For the $h_d = 2.9$ mm plate, variation of f_f is minimal with increasing Re .

In general, f_f is a weak function of Re .

Effect of Changing Clearance

Because there is only a small change in f_f with changes in Reynolds numbers, averaged (over the Re range) \bar{f}_f values will be used in some of the following comparisons. Figure 6(a) showing continuous increase in \bar{f}_f with increasing C_{pl} for all the test cases. Testing with water, Nava [7] reported a plateau clearance where f_f ceases to increase with increasing C_{pl} . Kheireddin [1] observed the same trend in all his tests. Note that the plateau clearance value reported by Nava was 0.762 mm (30 mils), but the maximum tested clearance in the current study as well as in Kheireddin's study was 0.635 mm (25 mils).

Childs and Fayolle [5] observed a similar trend of increasing friction factor with increasing clearance while testing liquid annular seals in a dynamic rig and incorporated this variation in predicting rotordynamic coefficients using a suitable model, instead of using the customary Blasius model which suggests that the friction factor is only a function of Re .

Effect of Changing Inlet Pressure

\bar{f}_f data are plotted versus P_{in} for all h_d and C_{pl} combinations in Fig.6(b), showing almost straight lines in all the cases. Inlet pressure has minimal effect on \bar{f}_f in the plates with $h_d = 0.9$ mm and 1.9 mm. In most cases, \bar{f}_f decreases slightly with increasing P_{in} . For $h_d = 2.9$ mm and $C_{pl} = 0.254$ mm, \bar{f}_f is considerably affected by changes in P_{in} . In this case, the test with $P_{in} = 56$ bar gives higher values of \bar{f}_f than the tests with $P_{in} = 84$ bar and 70 bar.

Effect of Changing Hole Depth

Figure.6 (c) shows Re based averaged f_f versus h_d . From 0.9 mm deep plates to 1.9 mm deep plates, f_f increases, and the increase gets steeper with increasing C_{pl} . From 1.9 mm to 2.9 mm, f_f decreases, leaving the situation hard to predict for other hole depths. But, this fluctuating tendency is maintained at all clearances and inlet pressures. Similar observations were made in Kheireddin [1].

Effect of Changing Hole Diameter

Kheireddin [1] had reported Darcy-Weisbach friction factor for the plates with 3.175 mm HP diameter. The current Fanning friction factor data with 12.15 mm HP diameter plates are multiplied by a factor of 4 for directly comparing them with Kheireddin's results.

One-on-one comparison cannot be made on these data, as changes in h_d affects f_f in different ways in addition to the effect of diameter. Hence, changes in f_f cannot be separately attributed to the effect of h_ϕ or h_d . Still, the data are plotted together to provide some comparison basis.

Friction factor data at each clearance for the tests with $P_{in} = 84$ bar are plotted for both of hole-patterns in Fig. 7 and support the following observations:

- At all clearances tested, the lowest friction factor corresponds to 12.15 mm plate, and the highest friction factor corresponds to 3.175 mm plate.
- At $C_{pl} = 0.254$ mm, the 3.175mm-hole-diameter plates have higher f_f values than 12.15mm-hole-diameter plates.
- At $C_{pl} = 0.381$ mm and 0.635 mm, the plates have comparable friction factor values.

To generalize, at the minimum clearance, plates with the smaller-hole pattern leak less than plates with larger hole diameters. When the clearance increases, this effect diminishes, and their leakage control is comparable.

Villasmil [8] used a commercial CFD code to predict friction factor for surfaces with recess patterns of different hole diameters (recesses were named Big, Large, Small, and Tiny based on hole diameter size in the decreasing order) with water as the medium. Some of his predictions were:

- The tiny recess (TR) emerges as the pattern with the highest friction factor in every clearance, with the exception of the 50 mils (1.270 mm).
- The big recess (BR) has the lowest friction factor for all clearances.
- The friction factor curves of the largest clearance (50 mils, 1.270 mm) in the small and tiny recesses are nearly equal for Reynolds number larger than 10,000.

Similar trends in f_f were also found in these experimental results, despite the fact that the recess patterns used in Villasmil's predictions had an area ratio significantly lower than the current plates and the medium used was water.

Dynamic pressure data

Ha [3] used his dynamic pressure measurements to explain friction-factor jump as a cavity-flow excitation phenomenon. In the current tests, friction factor jump was not observed. Still, for reference, dynamic pressure data in one of the tested configurations are presented in Fig. 8.

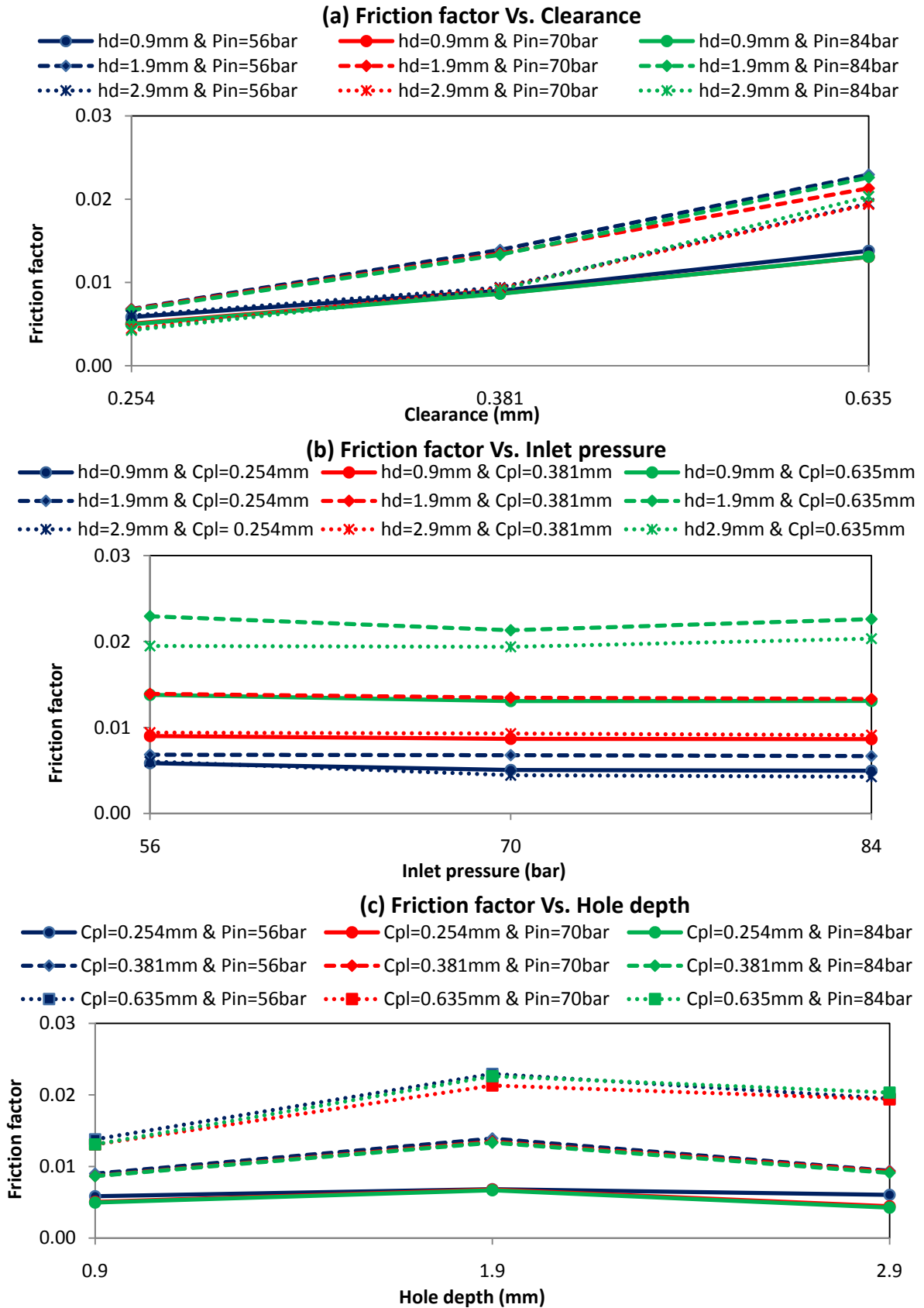


Figure 6. f_f versus (a) C_{pl} , (b) P_{in} , and (c) h_d

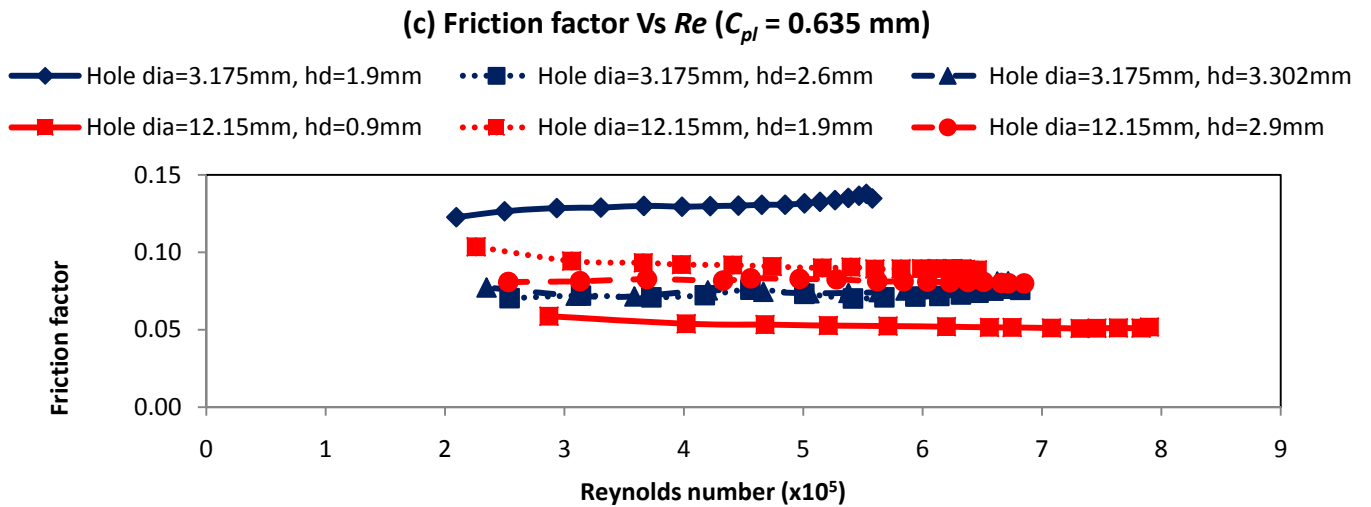
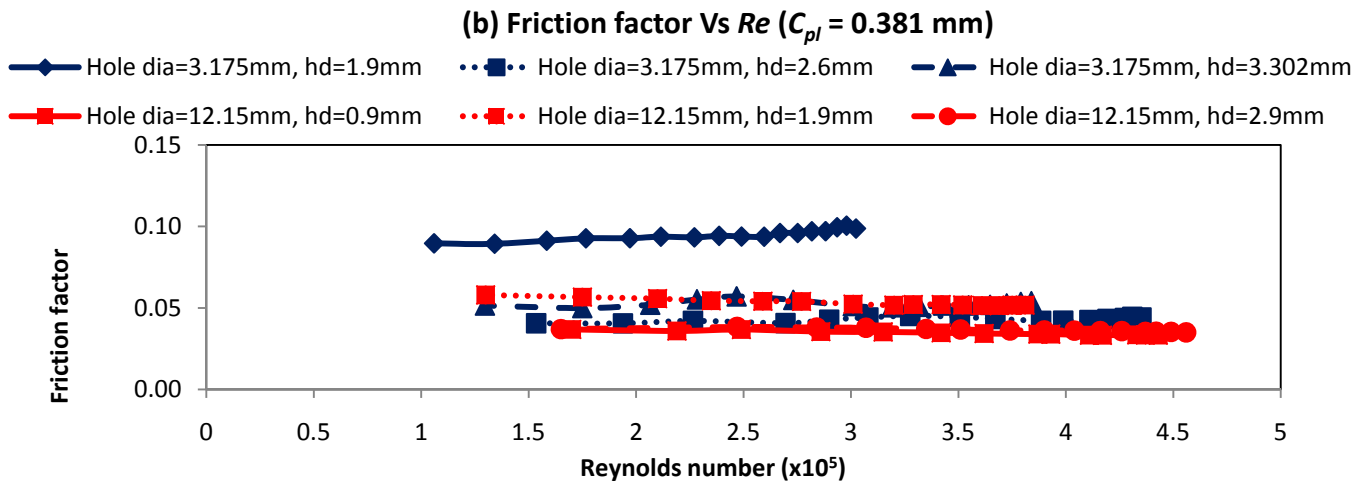
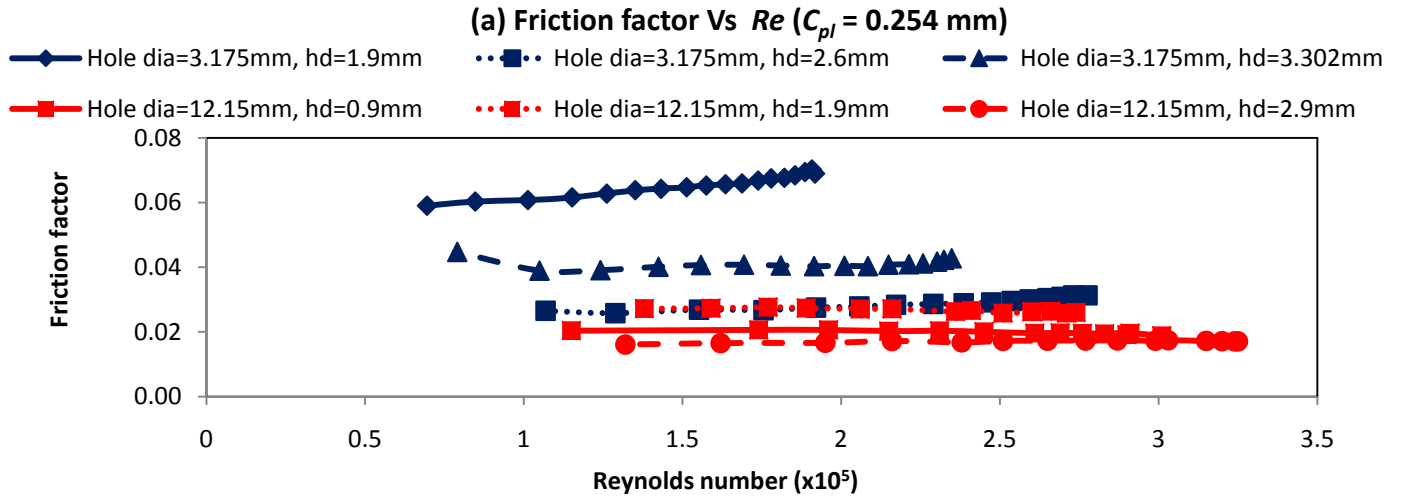


Figure 7. Comparison of Darcy-Weisbach f_f for plates with $h_p = 12.15$ mm and 3.175 mm at (a) $C_{pl} = 0.254$, (b) $C_{pl} = 0.381$, and (c) $C_{pl} = 0.635$ mm

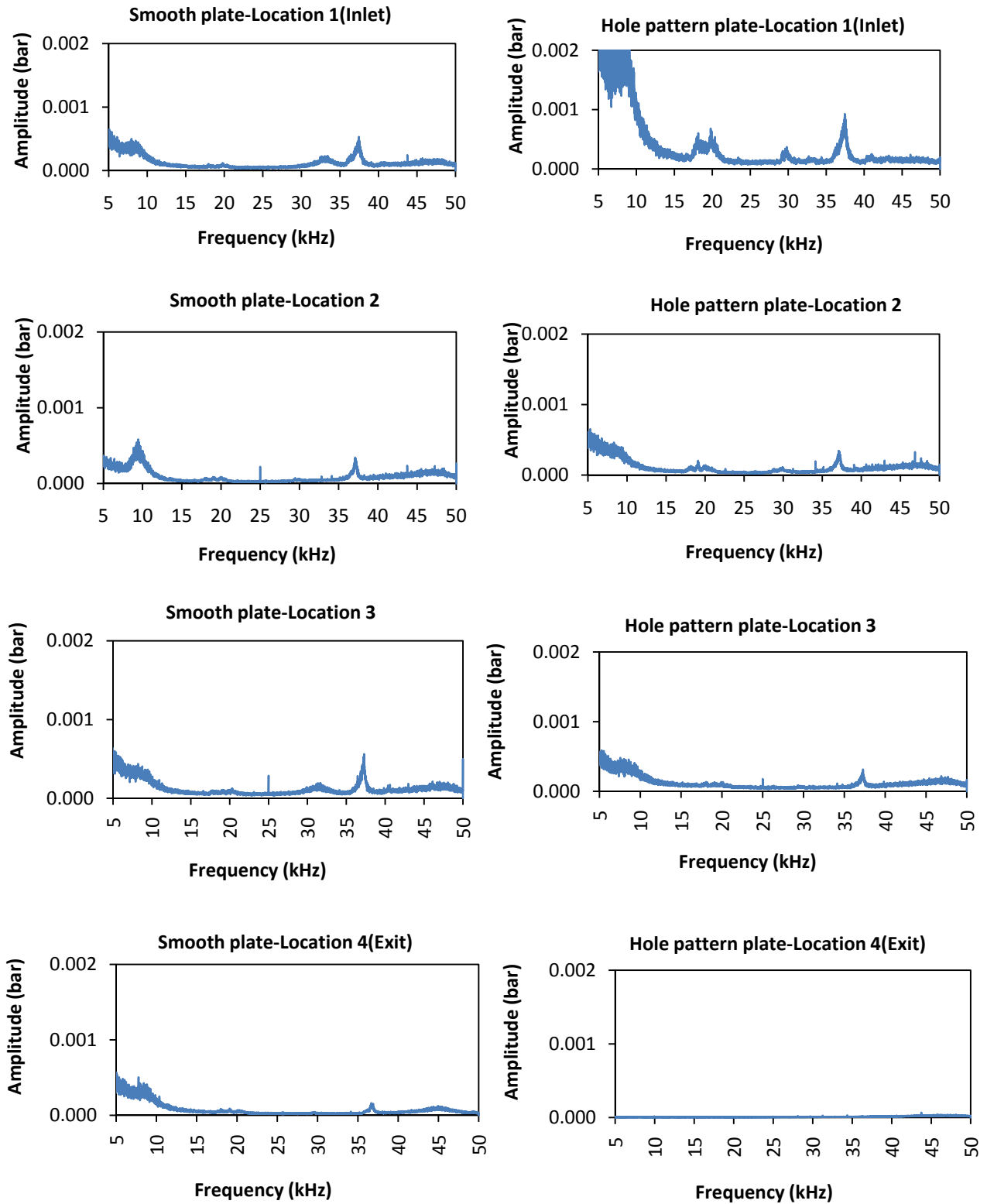


Figure 8. Dynamic pressure data spectra with $h_d = 2.9$ mm, $C_{pl} = 0.254$ mm, $P_{in} = 84$ bar, $Re = 32500$ (maximum)

From Fig. 8, measurements in both the smooth plate and HP plate show the dominant-component frequency lying between 35kHz and 40kHz. The pulsation magnitude is greater at the inlet and decreases gradually towards the exit. The dominant frequency is identical at the same axial location in both plates. The amplitude is greater on the HP side close to the inlet. Similar trends are observed in other test cases.

A complete uncertainty analysis and results for the test apparatus is provided in [2]. Reference [9] provides tabular friction-factor values at all tested configurations, dynamic pressure data for other configurations, and uncertainty calculations. (The maximum uncertainty in f_f was calculated to be 2.5%).

SUMMARY AND CONCLUSIONS

Three flat-plates with hole-pattern diameter 12.15 mm and hole depths of 0.9, 1.9, and 2.9 mm were tested with three clearance and three inlet-pressure combinations, thereby making nine tests for each plate. Friction factor data in all the tested configurations are presented.

Friction-factor jump is not observed in any of the tests, continuing the outcome reported by Childs et al. for HP surfaces apposed to smooth surfaces.

In comparison to results from Childs et al., the 3.175mm-hole-diameter plates have better leakage control than 12.15mm hole-diameter plates. The advantage diminishes when the clearance increases, and their leakage control performance is comparable.

Friction factor increases in moving from a hole depth of 0.9 mm to a hole depth of 1.9 mm and then decreases for a hole depth of 2.9 mm. This variable nature is observed in all test clearances and all inlet pressures. Similar observations have been made with honeycomb plates and plates with smaller diameter hole-pattern.

Friction factor is significantly affected by clearance. It increases continuously with increasing clearance within the tested clearance range. No plateau clearance was observed as reported by Nava. Previously tested honeycomb plates and small diameter holed plates also exhibited similar behavior.

For the ranges of data considered, changes in Reynolds number have a minimal impact on friction factor. In all test cases, friction factor either continuously decreases or remains almost constant with increasing Reynolds number.

Inlet pressure does not significantly affect friction factor. At low clearances, tests at low input pressure resulted in higher friction-factor values.

REFERENCES

- [1] Kheireddin, B., "Investigation of the Friction Factor Behavior for Flat Plates of Smooth and Roughened Surfaces with Supply Pressure up to 84 Bars," M.S. Thesis, Texas A&M Department of Mechanical Engineering, August 2009.
- [2] Childs, D., Philips, S., Kheireddin, B., and Deva Asirvatham, T., 2010, "Friction Factor Behavior from Flat-Plate Tests of Smooth and Hole-Pattern Roughened Surfaces with Supply Pressures Up To 84 Bars", *ASME Turbo Expo 2010*, GT 2010-22227.
- [3] Ha, T-W., Childs, D., 1992, "Friction-Factor Data for Flat-Plate Tests of Smooth and Honeycomb Surfaces," *ASME Trans., J. of Tribology*, **114**, pp. 722-730.
- [4] Kleynhans, G., and Childs, D., 1996, "The Acoustic Influence of Cell Depth on the Rotordynamic Characteristics of Smooth-Rotor/Honeycomb-Stator Annular Gas Seals," *ASME Journal of Engineering for Gas Turbines and Power*, 119, pp. 949-957.
- [5] Childs, D., and Fayolle, P., 1999, "Test Results for Liquid 'Damper' Seals using a Round-Hole Roughness Pattern for the Stators," *ASME Trans., Journal of Tribology*, **121**, pp. 42-49.
- [6] John, J., and Keith, T., 2006, *Gas Dynamics*, Prentice Hall. ISBN: 9780131206687.
- [7] Nava, D., 1993, "Observations of Friction Factors for Various Roughness Patterns in Channel Flow," MS Thesis, Department of Mechanical Engineering, Texas A&M University, College Station, TX.
- [8] Villasmil, L., Chen, H-C., and Childs, D., 2005, "Understanding Friction-Factor Behavior in Liquid annular Seals with Deliberately Roughened Surfaces," *AIAA Journal*, **43**, Number 10, pp. 2137-2146.
- [9] Deva Asirvatham, T., "Friction Factor Measurement, Analysis, and Modeling for Flat-Plates with 12.15 mm Diameter Hole-Pattern, Tested with Air at Different Clearances, Inlet Pressures, and Pressure Ratios," M.S. Thesis, Texas A&M Department of Mechanical Engineering, December 2010.